Symmetric joint measurement as a complement to the elegant joint measurement

Ying-Qiu He,[1] Yu-Yan Zhang,[1] Dong Ding,[1,2,*] Ting Gao,[3,†] and Feng-Li Yan[4,‡]

[1]*School of Science, University of Emergency Management, Beijing 101601, China*
[2]*Key Laboratory of Brain-Computer Interface Technology Application of the Ministry of Emergency Management, Beijing 101601, China*
[3]*School of Mathematical Sciences, Hebei Normal University, Shijiazhuang 050024, China*
[4]*College of Physics, Hebei Key Laboratory of Photophysics Research and Application, Hebei Normal University, Shijiazhuang 050024, China*

(Received 14 February 2026; accepted 13 August 2026; published 1 September 2026)

Traditional Bell state measurement (BSM) and the product basis measurement (PBM) have been integral to nearly the entire development of quantum computing. Unlike the BSM and the PBM, a recently proposed two-qubit joint measurement called the elegant joint measurement (EJM) exhibits novel tetrahedral symmetry in its single-qubit reduced states. In Tavakoli *et al.* [Phys. Rev. Lett. **126**, 220401 (2021)], a parametrized two-qubit isoentangled basis was proposed, with concurrence between 1/2 and 1, perfectly spanning the original EJM and conventional BSM. We present a two-qubit symmetric joint measurement having concurrence from 0 to 1/2, which is complementary to the parametrized EJM and connects the PBM and the original EJM. We investigate the symmetry of the current structure and its application in triangular networks. The results indicate that the reduced vectors of the current basis states exhibit rotational symmetry rather than mirror symmetry; moreover, the output probability distributions of three parties in the network explicitly demonstrate the expected permutation symmetry. Furthermore, we generalize the two-qubit symmetric joint measurement to the multiqubit systems with an even number of qubits.

DOI: 10.1103/dmhd-b7cd

I. INTRODUCTION

Quantum measurement serves as a fundamental component in quantum information processing [1–3], functioning as a crucial bridge between quantum resources and classical information. The inherent uncertainty in measurement outcomes underpins the unique advantages of quantum computing, enabling phenomena such as quantum parallelism [4]. A fundamental measurement operation in quantum information is the single-qubit measurement [5], typically performed as a projective measurement in a specific orthogonal basis (such as the computational basis $|0\rangle, |1\rangle$). In contrast to single-qubit measurements, multiqubit joint measurements are capable of projecting multiple qubits simultaneously. It reveals global system properties, such as network nonlocality [6–11] via correlated measurements typified by the Bell state measurement (BSM).

In 2019, Gisin [12] introduced a novel two-qubit isoentangled basis named the elegant joint measurement (EJM). For the four basis states of EJM, each has a concurrence of $C = 1/2$, and their single-qubit reduced states exhibit tetrahedral symmetry. Subsequently, Tavakoli *et al.* [13] generalized the original EJM to a single-parameter version that includes the traditional BSM. More recently, He *et al.* [14] further extended the single-parameter EJM to a three-parameter EJM, parametrized by z, φ, and θ. Ding *et al.* [15] explored the extension of the two-qubit EJM to multiqubit systems based on the three-parameter EJM. Concurrently, Del Santo *et al.* [16] offered a complete classification of two-qubit isoentangled joint measurement bases, and Pauwels *et al.* [17,18] utilized the tetrahedral directions involved in the original EJM as basic units to explore the construction of multiqubit joint measurements.

Let us now return to the subject of the two-qubit symmetric joint measurements. Consider the two-qubit state defined in Ref. [14],

$$|\Phi\rangle = \frac{1}{2\sqrt{2}}[(\sqrt{3}+e^{i\theta})|m_0, m_1\rangle + (\sqrt{3}-e^{i\theta})|m_1, m_0\rangle], \tag{1}$$

where the real parameter $\theta \in [0, \pi/2]$ and $\{|m_0\rangle, |m_1\rangle\}$ is a single-qubit orthogonal basis. Based on this state, a family of two-qubit EJM bases can be constructed, containing the single-parameter EJM. Nevertheless, we note that nearly all existing parametrized EJMs are confined to an achievable concurrence of $C = [1/2, 1]$. We are interested in whether, beyond this restriction, there exist other possibilities for constructing symmetric joint measurements. In this work, we redefine a two-qubit symmetric joint measurement basis. It serves as a complement to the EJMs, spanning the concurrence interval $C = [0, 1/2]$. We investigate the symmetry of the reductions of the current basis states and elucidate its relationship to the original EJM. As an application, we utilize this basis to detect network correlations in a triangular network, showing the permutation invariance of the resulting probability distributions. Finally, we extend the two-qubit symmetric joint measurement to multiqubit cases involving an even number of qubits.

*Contact author: dingdong@ncist.edu.cn
†Contact author: gaoting@hebtu.edu.cn
‡Contact author: flyan@hebtu.edu.cn

II. TWO-QUBIT SYMMETRIC JOINT MEASUREMENT BASIS

A. Definition of the basis states

We consider a two-qubit symmetric joint measurement, which differs from the recently proposed single- or three-parameter EJMs whose concurrences lie in the interval [1/2, 1]. To achieve this, we first define two single-qubit states,

$$|m_{k,0}\rangle = \frac{1}{\sqrt{2}}(\mathrm{e}^{-\mathrm{i}\pi/8}|m_k\rangle + \mathrm{e}^{\mathrm{i}\pi/8}|-m_k\rangle) \tag{2}$$

and

$$|m_{k,1}\rangle = \frac{1}{\sqrt{2}}(\mathrm{e}^{\mathrm{i}\pi/8}|m_k\rangle + \mathrm{e}^{-\mathrm{i}\pi/8}|-m_k\rangle), \tag{3}$$

where

$$|\pm m_k\rangle = \frac{1}{\sqrt{2}}[\sqrt{1\pm\cos(k\pi)}\mathrm{e}^{-\mathrm{i}\varphi_k/2}|0\rangle \pm \sqrt{1\mp\cos(k\pi)}\mathrm{e}^{\mathrm{i}\varphi_k/2}|1\rangle], \quad k=0,1,2,3, \tag{4}$$

with $\varphi_0=\varphi, \varphi_1=\varphi+\pi/2, \varphi_2=\varphi+\pi, \varphi_3=\varphi-\pi/2$, and the real parameter $\varphi\in[-\pi,\pi]$. Note that the states $|m_k\rangle$ and $|-m_k\rangle$ are orthogonal, $|m_{k,0}\rangle$ and $|m_{k,1}\rangle$ are nonorthogonal, i.e., $\langle m_k|-m_k\rangle = 0$ and $\langle m_{k,0}|m_{k,1}\rangle = 1/\sqrt{2}$.

We now define a set of two-qubit basis states,

$$|\Phi_k\rangle = \tfrac{1}{2}[(1+\mathrm{e}^{\mathrm{i}\theta})|m_{k,0},m_{k,1}\rangle + (1-\mathrm{e}^{\mathrm{i}\theta})|m_{k,1},m_{k,0}\rangle], \quad k=0,1,2,3, \tag{5}$$

where $|m_{k,0},m_{k,1}\rangle = |m_{k,0}\rangle\otimes|m_{k,1}\rangle$, for instance, and $\theta\in[0,\pi/2]$ is a real parameter. One can observe that when $\theta=0$, these basis states are clearly product states $|\Phi_k(\theta=0)\rangle = |m_{k,0},m_{k,1}\rangle$. Substituting states (2)–(4) into (5), the present basis states in the computational basis can be expressed as

$$|\Phi_k\rangle = \tfrac{1}{2}(\mathrm{e}^{-\mathrm{i}\varphi_k}|00\rangle - r^-_{k,\theta}|01\rangle - r^+_{k,\theta}|10\rangle + \mathrm{e}^{\mathrm{i}\varphi_k}|11\rangle), \tag{6}$$

where $r^\pm_{k,\theta} = [\cos(k\pi)\pm\mathrm{i}\mathrm{e}^{\mathrm{i}\theta}]/\sqrt{2}$. The orthogonality of these basis states is easily verified, i.e.,

$$\langle\Phi_j|\Phi_k\rangle = \tfrac{1}{4}[1+2\cos(\varphi_k-\varphi_j)+\cos(j\pi)\cos(k\pi)] = \delta_{jk}, \quad j,k=0,1,2,3. \tag{7}$$

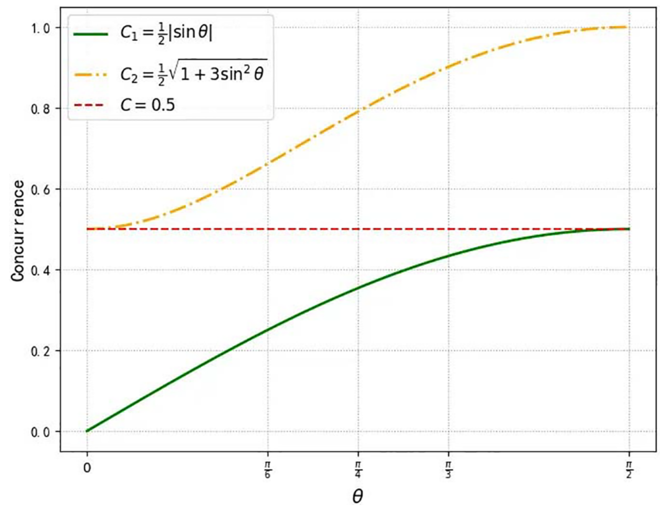

FIG. 1. Comparison of concurrence for the current states (green solid line) and previous parametrized EJMs (orange dashed-dotted line). Both vary with the parameter θ, distributed below and above $C=0.5$ (red dashed line, corresponding to the original EJM without parameters), respectively.

In comparison with state (1), this state differs in two respects: (i) the states $|m_{k,0}\rangle$ and $|m_{k,1}\rangle$ are not orthogonal, and (ii) the coefficients differ from those of the original state.

B. Symmetry

Typical symmetries of the EJM basis states are reflected in isoentanglement measures and the symmetry relations between their reduced states. We first calculate the concurrence [2] using $C=\sqrt{2(1-\mathrm{tr}\,\rho^2)}$, where ρ is a reduced state obtained by tracing out one qubit. A direct calculation gives

$$C(|\Phi_k\rangle) = \tfrac{1}{2}|\sin\theta|. \tag{8}$$

This is a nontrivial result with $C\in[0,1/2]$, which is distinct from the single- or three-parameter EJM cases, where the concurrence is given by $C=(1/2)\sqrt{1+3\sin^2\theta}\in[1/2,1]$. Therefore, it can serve as a complement to the previous parametrized EJMs. The combination of the previous EJM basis states and our current basis states yields an entanglement measure that fully covers the [0, 1] interval, as shown in Fig. 1.

We next see the reduced states of these basis states by calculate inner products $\langle\Phi_k|\vec{\sigma}\otimes I|\Phi_k\rangle$ and $\langle\Phi_k|I\otimes\vec{\sigma}|\Phi_k\rangle$. Here, $\vec{\sigma}=(\sigma_x,\sigma_y,\sigma_z)$ is the vector of Pauli matrices, where $\sigma_x,\sigma_y,\sigma_z$ are three Pauli observables. The calculation yields

$$\langle\Phi_k|\vec{\sigma}\otimes I|\Phi_k\rangle = \frac{1}{\sqrt{2}}\Big(-\cos(k\pi)\cos\varphi_k+\cos\theta\sin\varphi_k, -\cos(k\pi)\sin\varphi_k-\cos\theta\cos\varphi_k, \frac{1}{\sqrt{2}}\cos(k\pi)\sin\theta\Big) \tag{9}$$

and

$$\langle\Phi_k|I\otimes\vec{\sigma}|\Phi_k\rangle = \frac{1}{\sqrt{2}}\Big(-\cos(k\pi)\cos\varphi_k-\cos\theta\sin\varphi_k, -\cos(k\pi)\sin\varphi_k+\cos\theta\cos\varphi_k, -\frac{1}{\sqrt{2}}\cos(k\pi)\sin\theta\Big). \tag{10}$$

These two vectors are not mirror images of each other. Instead, they are connected through rotational symmetry. Either vector can be obtained by rotating the other by 180° around the axis defined by the vector $(\cos\varphi_k, \sin\varphi_k, 0)$, i.e., a line in the xy

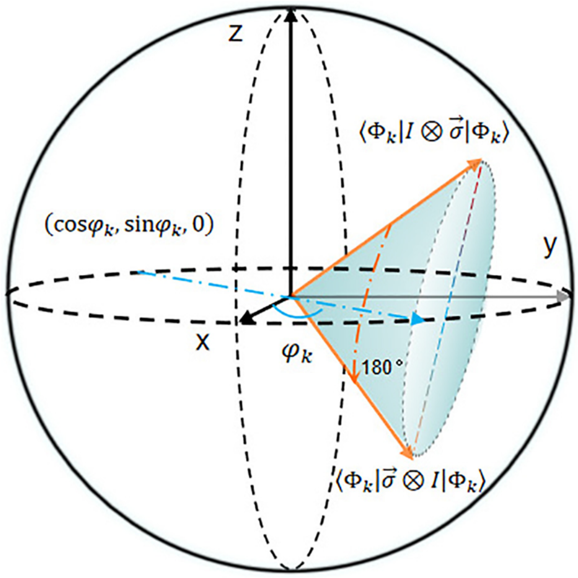

FIG. 2. Rotational symmetry of the vectors corresponding to the reduced states $\langle\Phi_k|\vec{\sigma}\otimes I|\Phi_k\rangle$ and $\langle\Phi_k|I\otimes\vec{\sigma}|\Phi_k\rangle$. One vector can be transformed into the other by a 180° rotation about the axis $(\cos\varphi_k, \sin\varphi_k, 0)$.

plane inclined at an angle φ_k to the x axis, as shown in Fig. 2.

More specifically, let $\vec{a}_k = \langle\Phi_k|\vec{\sigma}\otimes I|\Phi_k\rangle$ and $\vec{b}_k = \langle\Phi_k|I\otimes\vec{\sigma}|\Phi_k\rangle$, $k = 0, 1, 2, 3$. The end points of the four vectors $\vec{a}_k$ (or $\vec{b}_k$) form a tetrahedron, in which the two edges $|\vec{a}_0 - \vec{a}_2| = |\vec{a}_1 - \vec{a}_3| = \sqrt{2 + 2\cos^2\theta}$, while the other four edges are of length $\sqrt{2 + 2\cos\theta}$ (and likewise for $\vec{b}_k$). The four vertices of one tetrahedron can be transformed into those of the other by a rotation about their own axes. $\vec{b}_0$ and $\vec{b}_2$ result from rotating $\vec{a}_0$ and $\vec{a}_2$ by 180° around the axis $(\cos\varphi, \sin\varphi, 0)$, respectively, whereas $\vec{b}_1$ and $\vec{b}_3$ result from rotating $\vec{a}_1$ and $\vec{a}_3$ by 180° around the axis $(\sin\varphi, -\cos\varphi, 0)$. As a special case, when $\theta = \pi/2$ (for arbitrary φ), our results correspond to two regular tetrahedra that are mirror images of each other. In this case, the tetrahedra have an edge length of $\sqrt{2}$, and the vertices map as follows: $\vec{a}_0 \leftrightarrow \vec{b}_2$, $\vec{a}_1 \leftrightarrow \vec{b}_3$, $\vec{a}_2 \leftrightarrow \vec{b}_0$, $\vec{a}_3 \leftrightarrow \vec{b}_1$.

C. Relation to the original EJM basis

We next investigate the intrinsic connection between the current basis and the original EJM, which has a concurrence of $C = 1/2$. To do this, we set $\theta = \pi/2$, and the current basis states reduce to the following basis states,

$$|\Phi_k(\theta = \pi/2)\rangle = \tfrac{1}{2}(e^{-i\varphi_k}|00\rangle - r_k^+|01\rangle - r_k^-|10\rangle + e^{i\varphi_k}|11\rangle), \quad k = 0, 1, 2, 3, \tag{11}$$

where $r_k^\pm = [\cos(k\pi) \pm 1]/\sqrt{2}$, i.e., $r_k^\pm = 0$ or $\pm\sqrt{2}$. Also, we rewrite the original EJM basis up to a global phase factor as

$$|\Psi_k\rangle = \begin{cases} \frac{1}{2}(e^{-i\phi_k}|00\rangle - \sqrt{2}|01\rangle - e^{i\phi_k}|11\rangle), & k = 0, 2, \\ \frac{1}{2}(e^{-i\phi_k}|00\rangle + \sqrt{2}|10\rangle - e^{i\phi_k}|11\rangle), & k = 1, 3, \end{cases} \tag{12}$$

where $\phi_0 = \pi/4$, $\phi_1 = 3\pi/4$, $\phi_2 = -3\pi/4$, $\phi_3 = -\pi/4$. To clearly demonstrate the connection between these two bases, here we take $\varphi = \pi/4$, corresponding to $\varphi_k = \phi_k$. Compared to the original EJM, in addition to having equal entanglement measures, they exhibit the following connections: (i) Their single-qubit reduced states are identical; the vectors $\vec{a}_k$ and $\vec{b}_k$ (for $k = 0, 1, 2, 3$) form two mirror-image regular tetrahedra with radius $\sqrt{3}/2$. (ii) There exist orthogonality relations between the two bases, i.e., $\langle\Phi_{0,2}(\theta = \pi/2)|\Psi_{1,3}\rangle = \langle\Phi_{1,3}(\theta = \pi/2)|\Psi_{0,2}\rangle = 0$. (iii) These two bases share the same probability distribution in the computational basis, but are distinguished by a relative phase induced by a controlled-Z operation, namely, $|\Psi_k\rangle = \mathrm{CZ}|\Phi_k(\theta = \pi/2)\rangle$.

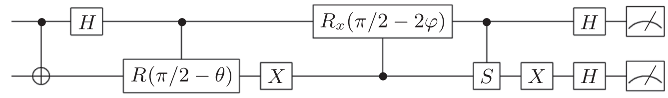

FIG. 3. Quantum circuit for the current symmetric joint measurement.

D. Quantum circuits

We here provide the quantum circuit for the current symmetric joint measurement, as shown in Fig. 3. Our quantum circuit incorporates the conventional single-qubit gates $H = (\sigma_x + \sigma_z)/\sqrt{2}$ and $X = \sigma_x$, as well as available two-qubit controlled gates: $C_{R(\pi/2-\theta)}$, $C_{R_x(\pi/2-2\varphi)}$, controlled-NOT (CNOT) and the controlled-phase gate. Here, $R(\pi/2 - \theta) = \mathrm{diag}[1, e^{i(\pi/2-\theta)}]$, $S = R(\pi/2)$, and $R_x(\pi/2 - 2\varphi) = e^{-i(\pi/4-\varphi)\sigma_x}$. In this way, the four orthonormal basis states of the current symmetric joint measurement can be discriminated

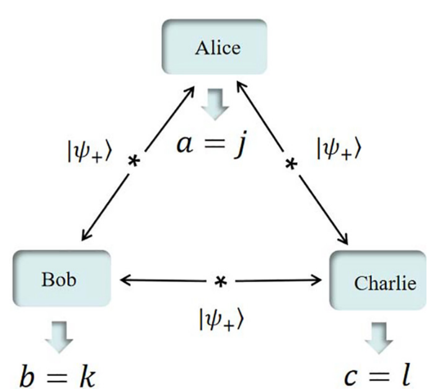

FIG. 4. A triangular network of three parties connected by three independent sources. Each source creates a pair of Bell states $|\psi_+\rangle = (|01\rangle + |10\rangle)/\sqrt{2}$, which are distributed to neighboring parties. All parties perform the current symmetric joint measurements; the outputs for Alice, Bob, and Charlie are denoted by a, b, and c, respectively.

in the computational basis, as

$$|\Phi_0\rangle \to |01\rangle,\ |\Phi_1\rangle \to -|11\rangle,$$
$$|\Phi_2\rangle \to -|00\rangle,\ |\Phi_3\rangle \to |10\rangle. \tag{13}$$

In contrast to the previous quantum circuits [13,14], we incorporate two-qubit controlled gates [namely, the $C_{R_x(\pi/2-2\varphi)}$ gate and the controlled-S (CS) gate] to evolve the composite quantum system. When $\varphi = \pi/4$ [such that $R_x(\pi/2 - 2\varphi) = I$], the current measurement reduces to a single-parameter symmetric joint measurement with a concurrence of $C \in [0, 1/2]$. Moreover, at $\theta = \pi/2$, the term $R(\pi/2 - \theta)$ becomes I, thereby recovering the original EJM [12] corresponding to $\theta = 0$ in the previous circuit [13] up to local unitary transformations.

III. APPLICATION

Here, we apply the current symmetric joint measurement basis to the triangular network, as shown in Fig. 4. We assume that three independent sources each prepares a pair of Bell states $|\psi_+\rangle = (|01\rangle + |10\rangle)/\sqrt{2}$ and distributes them to the neighboring parties Alice and Bob, Bob and Charlie, and Charlie and Alice, respectively. The composite system reads

$$|\Psi_{ABC}\rangle = |\psi_+\rangle_{A_2B_1} \otimes |\psi_+\rangle_{B_2C_1} \otimes |\psi_+\rangle_{C_2A_1}. \tag{14}$$

Then, the joint probability corresponding to network parties Alice, Bob, and Charlie resulting in $|\Phi_j\rangle_{A_1A_2}$, $|\Phi_k\rangle_{B_1B_2}$, and $|\Phi_l\rangle_{C_1C_2}$, respectively, is

$$p(a = j, b = k, c = l) = |\langle\Phi_{jkl}|\Psi_{ABC}\rangle|^2,\quad j, k, l = 0, 1, 2, 3, \tag{15}$$

where $|\Phi_{jkl}\rangle = |\Phi_j\rangle_{A_1A_2} \otimes |\Phi_k\rangle_{B_1B_2} \otimes |\Phi_l\rangle_{C_1C_2}$.

Calculate

$$\begin{aligned}\langle\Phi_{jkl}|\Psi_{ABC}\rangle = \frac{1}{32}\{&e^{-2i\theta}[\cos(j\pi) + \cos(k\pi) + \cos(l\pi)] + 2e^{-i\theta}[\sin(\phi_j - \phi_k) + \sin(\phi_k - \phi_l) + \sin(\phi_l - \phi_j)]\\ &- 2[\cos(j\pi)\cos(\phi_k - \phi_l) + \cos(k\pi)\cos(\phi_l - \phi_j) + \cos(l\pi)\cos(\phi_j - \phi_k)]\\ &- \cos(j\pi)\cos(k\pi)\cos(l\pi)\}.\end{aligned} \tag{16}$$

Then we have

$$p(a = j, b = k, c = l) = \begin{cases} \dfrac{4 + 21\sin^2\theta}{256}, & \text{if } j = k = l,\\ \dfrac{4 + \sin^2\theta}{256}, & \text{if } j \neq k \neq l \neq j,\\ \dfrac{4 - 3\sin^2\theta}{256}, & \text{else,}\end{cases} \tag{17}$$

satisfying the normalization condition

$$\tfrac{1}{256}[(4 + 21\sin^2\theta) \times 4 + (4 + \sin^2\theta) \times 24 + (4 - 3\sin^2\theta) \times 36] = 1. \tag{18}$$

It is observed that the output probabilities of the measurement results vary with the real parameter θ, always maintaining permutation invariance. In particular, for $\theta = \pi/2$, the probabilities simplify to those of the original EJM case: $p(a = b = c = j) = 25/256$, $p(a = j, b = k, c = l) = 5/256$ (where $j \neq k \neq l \neq j$), and $p(a = b = j, c = l) = 1/256$ for $j \neq l$, as well as their cyclic permutations. In contrast, for $\theta = 0$, the probabilities become uniform with $p = 1/64$, corresponding to all parties performing measurements in the product basis.

For the triangular network, Gisin [12] conjectured that the maximal three-particle trilocal correlation is $p_{\max}(a = b = c) = 61/256$. Once this bound is surpassed by the quantum system, the quantum probability $p(a, b, c)$ is arguably not trilocal. Here, a direct calculation results in

$$p(a = b = c) = \frac{4 + 21\sin^2\theta}{64}, \tag{19}$$

where notably such a trilocal model fails to reproduce the quantum correlations for $\arcsin(\sqrt{15/28}) < \theta \leqslant \pi/2$. This provides a parametrizable framework for the study of quantum correlations in triangle networks.

IV. MULTIQUBIT SYMMETRIC JOINT MEASUREMENT BASIS

In this section, we extend the current symmetric joint measurement basis to the even-n case. Concretely, for even n, an n-qubit symmetric joint measurement basis is defined as

$$|\Phi_{k_1\cdots k_{n/2}}\rangle = \tfrac{1}{2}[(1 + e^{i\theta})|m_{k_1,0}, m_{k_1,1}, \ldots, m_{k_{n/2},0}, m_{k_{n/2},1}\rangle + (1 - e^{i\theta})|m_{k_1,1}, m_{k_1,0}, \ldots, m_{k_{n/2},1}, m_{k_{n/2},0}\rangle], \tag{20}$$

where $k_1, \ldots, k_{n/2} = 0, 1, 2, 3$. To verify the orthonormality of the basis state, we calculate inner product

$$\begin{aligned}\langle\Phi_{j_1\cdots j_{n/2}}|\Phi_{k_1\cdots k_{n/2}}\rangle = \tfrac{1}{4}(&|1 + e^{i\theta}|^2\langle m_{j_1,0}|m_{k_1,0}\rangle\langle m_{j_1,1}|m_{k_1,1}\rangle\cdots\langle m_{j_{n/2},0}|m_{k_{n/2},0}\rangle\langle m_{j_{n/2},1}|m_{k_{n/2},1}\rangle\\ &+ |1 - e^{i\theta}|^2\langle m_{j_1,1}|m_{k_1,1}\rangle\langle m_{j_1,0}|m_{k_1,0}\rangle\cdots\langle m_{j_{n/2},1}|m_{k_{n/2},1}\rangle\langle m_{j_{n/2},0}|m_{k_{n/2},0}\rangle).\end{aligned} \tag{21}$$

To simplify the calculation, we here define two sets of orthonormal bases,

$$|m_0^{\pm}\rangle = \frac{1}{\sqrt{2}}[\mathrm{e}^{-\mathrm{i}(\varphi/2+\pi/8)}|0\rangle \pm \mathrm{e}^{\mathrm{i}(\varphi/2+\pi/8)}|1\rangle] \tag{22}$$

and

$$|m_1^{\pm}\rangle = \frac{1}{\sqrt{2}}[\mathrm{e}^{-\mathrm{i}(\varphi/2-\pi/8)}|0\rangle \pm \mathrm{e}^{\mathrm{i}(\varphi/2-\pi/8)}|1\rangle], \tag{23}$$

satisfying $\langle m_0^+|m_0^-\rangle = \langle m_1^+|m_1^-\rangle = 0$. Accordingly, $|m_{k,0}\rangle$ and $|m_{k,1}\rangle$ can be written as

$$\begin{aligned} &|m_{0,0}\rangle = |m_0^-\rangle,\ |m_{1,0}\rangle = |m_0^+\rangle, \\ &|m_{2,0}\rangle = -\mathrm{i}|m_0^+\rangle,\ |m_{3,0}\rangle = \mathrm{i}|m_0^-\rangle, \end{aligned} \tag{24}$$

and

$$\begin{aligned} &|m_{0,1}\rangle = |m_1^-\rangle, \quad |m_{1,1}\rangle = -\mathrm{i}|m_1^-\rangle, \\ &|m_{2,1}\rangle = -\mathrm{i}|m_1^+\rangle, \quad |m_{3,1}\rangle = |m_1^+\rangle. \end{aligned} \tag{25}$$

From this, we can immediately derive $\langle m_{j_1,0}|m_{k_1,0}\rangle\langle m_{j_1,1}|m_{k_1,1}\rangle = \delta_{j_1k_1}$, and thus we have

$$\langle \Phi_{j_1\cdots j_{n/2}}|\Phi_{k_1\cdots k_{n/2}}\rangle = \delta_{j_1k_1}\cdots\delta_{j_{n/2}k_{n/2}}, \quad j_1,\ldots,j_{n/2}, \quad k_1,\ldots,k_{n/2} = 0,1,2,3. \tag{26}$$

Therefore, the states (20) constitute an n-qubit orthogonal basis, which reduces to the previous two-qubit basis states (5) when $n = 2$. It is clear that the product bases are contained when $\theta = 0$.

The symmetry of these basis states is revealed by calculating the inner product $\langle \Phi_{k_1\cdots k_{n/2}}|(\vec{\sigma}\otimes I\otimes\cdots\otimes I)_{\mathrm{perm}}|\Phi_{k_1\cdots k_{n/2}}\rangle$, where $(\cdot)_{\mathrm{perm}}$ stands for all permutations of the operators. The results of the inner products are given by the following expression,

$$\begin{aligned} I_{k_i}^{\pm} = \tfrac{1}{2}[&(\langle m_{k_i,0}|\vec{\sigma}|m_{k_i,0}\rangle + \langle m_{k_i,1}|\vec{\sigma}|m_{k_i,1}\rangle) \pm \cos\theta(\langle m_{k_i,0}|\vec{\sigma}|m_{k_i,0}\rangle - \langle m_{k_i,1}|\vec{\sigma}|m_{k_i,1}\rangle) \\ &\mp 2^{\frac{1-n}{2}} \times \mathrm{i}\sin\theta(\langle m_{k_i,0}|\vec{\sigma}|m_{k_i,1}\rangle - \langle m_{k_i,1}|\vec{\sigma}|m_{k_i,0}\rangle)], \quad i = 1,2,\ldots,n/2. \end{aligned} \tag{27}$$

A not very complicated calculation yields

$$I_{k_i}^{\pm} = \frac{1}{\sqrt{2}}[-\cos(k_i\pi)\cos\varphi_{k_i} \pm \cos\theta\sin\varphi_{k_i}, -\cos(k_i\pi)\sin\varphi_{k_i} \mp \cos\theta\cos\varphi_{k_i}, \pm 2^{\frac{1-n}{2}}\cos(k_i\pi)\sin\theta]. \tag{28}$$

Therefore, the rotational symmetry of these reductions is preserved.

In contrast to the previous works [15,17,18], here we focus on constructing multipartite symmetric joint measurements that incorporate product bases. In particular, compared with the work of Pauwels *et al.* [17,18], in which they constructed multipartite EJMs using group orbits of a fiducial state under tensor-product actions of the generalized Pauli group, we place more emphasis on proposing continuously parametrized symmetric joint measurement bases whose entanglement measures can reach 0, and that can serve as a complement to the conventional EJMs.

V. DISCUSSION AND SUMMARY

In summary, we have proposed a two-qubit symmetric joint measurement, which differs from the previous single- or three-parameter EJMs whose concurrences lie in the interval [1/2, 1]. Although its expression is quite similar to the previous single-parameter EJM, its concurrence falls within [0, 1/2], making it an effective complement to the previous EJMs. By introducing a real parameter θ, the single-parameter EJM incorporates BSM and the original EJM; likewise, the current basis bridges product bases ($\theta = 0$) and the original EJM ($\theta = \pi/2$).

We have investigated the symmetry of the current basis states by analyzing the relationships between their single-qubit reductions. Distinct from the mirror symmetry of the reduced states in the previous EJMs, our derived reduced states feature rotational symmetry. In particular cases, such as $\theta = \pi/2$, this symmetry can degenerate to mirror symmetry. In applications, we apply the current symmetric joint measurement to a triangular network with three independent sources. As a result, this structure can not only reveal quantum network correlations, but the output probability distributions of the three parties also exhibit the expected permutation symmetry. Moreover, we have extended the two-qubit symmetric joint measurement to multiqubit systems consisting of an even number of qubits.

Several aspects of this work remain to be further improved. (1) The present symmetric joint measurement covers the same concurrence interval [0, 1/2] as the "elegant family" in Ref. [16]. It can be mapped to the elegant family via local transformations [19], yet the underlying mechanism connecting the two constructions remains elusive. (2) The rotational symmetry of the single-qubit reduced states found in this work is conceptually more general than the previous mirror symmetry. It remains an open question whether this rotational symmetry should be a primary consideration in future extensive studies of symmetry measurements. (3) In terms of applications, beyond the network nonlocality that has already been experimentally realized [20,21], it is worth asking whether there exist other applications capable of surpassing BSM. After all, in quantum teleportation using EJM [22], aside from offering a wider range of measurement settings, no more exciting results have been obtained. (4) We generalize two-qubit symmetric joint measurements to the multiqubit systems, specifically focusing on the even-number cases. While the strategy in Ref. [15] allows for the extension to odd-number cases, achieving a generalization for an arbitrary number of qubits or higher-dimensional systems [18,23] remains an open problem. These parametrized structures extend conceptual frameworks and enrich symmetric joint measurements, while offering different perspectives for future applications.

ACKNOWLEDGMENTS

We thank J. Czartowski and K. Życzkowski for stimulating correspondence and helpful discussions. This work was supported by the Hebei Science and Technology Program Foundation of China under Grant No. 246Z0902G.

DATA AVAILABILITY

There are no publicly available research data or software supporting this manuscript. Requests for further information or data should be sent to the authors.

[1] M. Hayashi, S. Ishizaka, A. Kawachi, G. Kimura, and T. Ogawa, *Introduction to Quantum Information Science* (Springer, Heidelberg, 2015).

[2] R. Horodecki, P. Horodecki, M. Horodecki, and K. Horodecki, Quantum entanglement, Rev. Mod. Phys. **81**, 865 (2009).

[3] O. Gühne and G. Tóth, Entanglement detection, Phys. Rep. **474**, 1 (2009).

[4] Edited by F. F. Fanchini, D. de Oliveira Soares Pinto, and G. Adesso, *Lectures on General Quantum Correlations and Their Applications*, Springer Series on Quantum Science and Technology (Springer, Cham, 2017).

[5] M. A. Nielsen and I. L. Chuang, *Quantum Computation and Quantum Information* (Cambridge University Press, Cambridge, 2000).

[6] C. Branciard, N. Gisin, and S. Pironio, Characterizing the nonlocal correlations created via entanglement swapping, Phys. Rev. Lett. **104**, 170401 (2010).

[7] A. Tavakoli, P. Skrzypczyk, D. Cavalcanti, and A. Acín, Nonlocal correlations in the star-network configuration, Phys. Rev. A **90**, 062109 (2014).

[8] N. Gisin, *Quantum Chance, Nonlocality, Teleportation and Other Quantum Marvels* (Springer, Berlin, 2014).

[9] M. X. Luo, Computationally efficient nonlinear Bell inequalities for quantum networks, Phys. Rev. Lett. **120**, 140402 (2018).

[10] A. Pozas-Kerstjens, N. Gisin, and A. Tavakoli, Full network nonlocality, Phys. Rev. Lett. **128**, 010403 (2022).

[11] A. Tavakoli, A. Pozas-Kerstjens, M. X. Luo, and M. O. Renou, Bell nonlocality in networks, Rep. Prog. Phys. **85**, 056001 (2022).

[12] N. Gisin, Entanglement 25 years after quantum teleportation: Testing joint measurements in quantum networks, Entropy **21**, 325 (2019).

[13] A. Tavakoli, N. Gisin, and C. Branciard, Bilocal Bell inequalities violated by the quantum elegant joint measurement, Phys. Rev. Lett. **126**, 220401 (2021).

[14] Y. Q. He, D. Ding, T. Gao, Z. J. Li, and F. L. Yan, Three-parameter symmetric quantum joint measurement on two qubits, Phys. Rev. A **111**, 012429 (2025).

[15] D. Ding, Y. Q. He, T. Gao, and F. L. Yan, Symmetric quantum joint measurements on multiple qubits, Phys. Rev. A **111**, 052450 (2025).

[16] F. Del Santo, J. Czartowski, K. Życzkowski, and N. Gisin, Iso-entangled bases and joint measurements, Phys. Rev. Res. **6**, 023085 (2024).

[17] J. Pauwels and N. Gisin, Multiqubit elegant joint measurement, Phys. Rev. Lett. **136**, 190201 (2026).

[18] J. Pauwels, C. Branciard, A. Pozas-Kerstjens, and N. Gisin, Symmetric localizable multipartite quantum measurements from Pauli orbits, Phys. Rev. A **113**, 052432 (2026).

[19] J. Czartowski and K. Życzkowski (private communication).

[20] E. Bäumer, N. Gisin, and A. Tavakoli, Demonstrating the power of quantum computers, certification of highly entangled measurements and scalable quantum nonlocality, npj Quantum Inf. **7**, 117 (2021).

[21] C. X. Huang, X. M. Hu, Y. Guo, C. Zhang, B. H. Liu, Y. F. Huang, C. F. Li, G. C. Guo, N. Gisin, C. Branciard, and A. Tavakoli, Entanglement swapping and quantum correlations via symmetric joint measurements, Phys. Rev. Lett. **129**, 030502 (2022).

[22] D. Ding, M. X. Yu, Y. Q. He, H. S. Ji, T. Gao, and F. L. Yan, Quantum teleportation based on the elegant joint measurement, Phys. Lett. A **527**, 129991 (2024).

[23] J. Czartowski and K. Życzkowski, Bipartite quantum measurements with optimal single-sided distinguishability, Quantum **5**, 442 (2021).